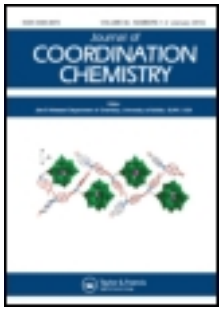

Journal of Coordination Chemistry
Publication details, including instructions for authors and subscription information:
http://www.tandfonline.com/loi/gcoo20

Syntheses, structures, and properties of a series of new assembled metal complexes with 4-(benzimidazol-1-ylmethyl)benzoate

Hai-Wei Kuai [a], Xiao-Chun Cheng [a] & Xiao-Hong Zhu [a]
[a] Faculty of Life Science and Chemical Engineering, Huaiyin Institute of Technology, Huaian, PR China
Accepted author version posted online: 07 Nov 2012.Published online: 10 Dec 2012.

To cite this article: Hai-Wei Kuai, Xiao-Chun Cheng & Xiao-Hong Zhu (2013) Syntheses, structures, and properties of a series of new assembled metal complexes with 4-(benzimidazol-1-ylmethyl)benzoate, Journal of Coordination Chemistry, 66:1, 28-41, DOI: 10.1080/00958972.2012.746458

To link to this article: http://dx.doi.org/10.1080/00958972.2012.746458

Journal of Coordination Chemistry
Vol. 66, No. 1, 10 January 2013, 28–41

Syntheses, structures, and properties of a series of new assembled metal complexes with 4-(benzimidazol-1-ylmethyl) benzoate

HAI-WEI KUAI*, XIAO-CHUN CHENG and XIAO-HONG ZHU

Faculty of Life Science and Chemical Engineering, Huaiyin Institute of Technology, Huaian, PR China

(*Received 29 January 2012; in final form 19 September 2012*)

A series of complexes based on 4-(benzimidazol-1-ylmethyl)benzoic acid (HL), $[Co(L)_2]\cdot H_2O$ (**1**), $[Zn(L)_2]\cdot H_2O$ (**2**), $[Mn(L)_2(phen)]\cdot H_2O$ (**3**), and $[Mn_2(L)_2(phen)_4]\cdot 2ClO_4$ (**4**) [phen = 1,10-phenanthroline], were synthesized under hydrothermal conditions and characterized by single-crystal and powder X-ray diffractions, IR, elemental, and thermogravimetric analyzes. HL features O-donor carboxylate and flexible N-donor benzimidazol-1-ylmethyl groups, allowing varied coordination and conformations. Complex **1** exhibits a uninodal 4-connected 2-D network structure with $(4^4.6^2)$ topology. Complex **2** has a similar 2-D architecture to **1**. Complex **3** consists of 2-D networks, displaying a uninodal 4-connected 2-D network with $(4^4.6^2)$ topology. Complex **4** shows a dinuclear structure, which can be further linked to form a 2-D layer through $C-H\cdots_{\pi}$ interactions. The results imply that metal centers, auxiliary ligand, and counter anions subtly influence the structure of resultant complexes. In addition, the fluorescence of **2** and magnetism of **4** have been examined.

Keywords: Cobalt; Zinc; Manganese; Metal-organic framework; Properties

1. Introduction

Crystal engineering of metal-organic frameworks (MOFs) with well-defined sizes and beautiful shapes has been achieved in supramolecular chemistry, coordination chemistry, and materials chemistry [1]. Interest in these fields is justified owing to intriguing architectures and potential applications as functional materials [2]. The aim of crystal engineering is to explore new crystalline materials with intriguing structures and interesting properties [3]. A number of MOFs have been reported [4], however, functional properties of complexes are largely dependent on architectures, and thus, the assembly of coordination compounds with variable structures seems to be significant for new crystalline materials. Previous studies have shown that solvent, reaction temperature, and ratio of metal-to-ligand can exert subtle influence on the assembly and structure of complexes [5]. The role of organic ligands is most important, providing an impetus to design ligands and construct MOFs under varied reaction conditions [6].

*Corresponding author. Email: kuaihaiwei@hyit.edu.cn

Journal of Coordination Chemistry
ISSN 0095-8972 print/ISSN 1029-0389 online
http://dx.doi.org/10.1080/00958972.2012.746458

Recently, we have focused our attention on new multidentate N – and O-donors: 4-(benzimidazol-1-ylmethyl)benzoic acid (HL) for building desirable frameworks. Our main goal is to investigate the influence of intrinsic features of HL and external conditions on the structures and properties of complexes. Compared with other N – or O-donors, HL possesses several distinctive features. First, HL is an aromatic carboxylate-containing ligand, and thus may participate in assembly of coordination polymers with various structures from variable bonding of carboxylate such as μ_1-$\eta^1:\eta^0$-monodentate and μ_2-$\eta^1:\eta^1$-briding modes [7]. Second, HL could adopt different molecular conformations in self-assembly with the flexible benzimidazol-1-ylmethyl group which could rotate to different degrees and thus have more spatial freedom to adopt different orientations to satisfy coordination requirements [8]. Third, the steric hindrance of benzimidazol-1-yl may induce structural evolution and maintain a specific configuration. Therefore, the variable coordination modes and conformations of HL provide the possibility to assemble complexes with various architectures by adjustments of reaction conditions including the presence of auxiliary ligand and alteration of metal centers and counter anions.

In this contribution, we describe the syntheses, structures, and properties of a series of new metal complexes with 4-(benzimidazol-1-ylmethyl)benzoate: $[Co(L)_2]\cdot H_2O$ (**1**), $[Zn(L)_2]\cdot H_2O$ (**2**), $[Mn(L)_2(phen)]\cdot H_2O$ (**3**), and $[Mn_2(L)_2(phen)_4]\cdot 2ClO_4$ (**4**). Complexes **1–4** have been characterized by single-crystal X-ray structure determination, FT-IR spectroscopy, elemental analysis, powder X-ray diffraction (PXRD), and thermogravimetric analyzes (TGA). Fluorescence of **2** and magnetism of **4** have been investigated. HL has not previously been employed as an organic block to assemble transition metal complexes.

2. Experimental

2.1. *Materials and methods*

Commercially available chemicals are of reagent grade and were used as received. A slightly revised experimental procedure was employed to synthesize HL [9]. C, H, and N analyzes were taken on a Perkin-Elmer 240C elemental analyzer. Infrared spectra (IR) were recorded on a Bruker Vector22 FT-IR spectrophotometer using KBr pellets. TGA were performed on a simultaneous SDT 2960 thermal analyzer under nitrogen with a heating rate of 10 °C min^{-1}. PXRD patterns were measured on a Shimadzu XRD-6000 X-ray diffractometer with Cu K_α ($\lambda = 1.5418$ Å) radiation at room temperature. Luminescence spectra for the powdered solid sample were measured on an Aminco Bowman Series 2 spectrofluorometer with a xenon arc lamp as the light source. For emission and excitation spectra, the pass width is 5 nm and all the measurements were carried out under the same experimental conditions. The magnetic measurement from 1.8 to 300 K was carried out on a Quantum Design MPMS7 SQUID magnetometer in a field of 2000 Oe.

2.2. *Preparation of $[Co(L)_2]\cdot H_2O$ (1)*

Reaction mixture of $Co(NO_3)_2\cdot 6H_2O$ (29.1 mg, 0.1 mmol), HL (25.2 mg, 0.1 mmol), and KOH (5.61 mg, 0.1 mmol) in 10 mL H_2O was sealed in a 16 mL Teflon-lined stainless steel container and heated at 140 °C for 3 days. After cooling to room temperature, dark purple block crystals of **1** were collected by filtration and washed by water and ethanol several

times with a yield of 52% based on HL. Anal. calcd for $C_{30}H_{24}N_4O_5Co$: C, 62.18; H, 4.17; N, 9.67%. Found: C, 61.96; H, 4.26; N, 9.42%. IR (KBr pellet, cm^{-1}): 3441 (m, br), 1609 (m), 1594 (s), 1549 (s), 1508 (s), 1462 (w), 1417 (s), 1392 (s), 1296 (w), 1260 (w), 1205 (w), 1114 (w), 1022 (w), 977 (w), 951 (w), 916 (w), 855 (m), 799 (m), 754 (s), 623 (w).

2.3. *Preparation of $[Zn(L)_2]\cdot H_2O$ (2)*

Reaction mixture of $Zn(NO_3)_2\cdot 6H_2O$ (29.7 mg, 0.1 mmol), HL (25.2 mg, 0.1 mmol), and KOH (5.61 mg, 0.1 mmol) in 10 mL H_2O was sealed in a 16 mL Teflon-lined stainless steel container and heated at 140 °C for 3 days. After cooling to room temperature, colorless block crystals of **2** were collected by filtration and washed by water and ethanol several times giving 31% yield based on HL. Anal. calcd for $C_{30}H_{24}N_4O_5Zn$: C, 61.49; H, 4.13; N, 9.56%. Found: C, 61.26; H, 3.86; N, 9.36%. IR (KBr pellet, cm^{-1}): 3432 (m, br), 1610 (s), 1560 (m), 1509 (m), 1469 (w), 1417 (m), 1382 (s), 1410 (s), 1297 (w), 1266 (w), 1206 (w), 1185 (m), 1134 (w), 1018 (w), 922 (w), 846 (w), 811 (w), 775 (m), 745 (s), 695 (w), 669 (w), 623 (w).

2.4. *Preparation of $[Mn(L)_2(phen)]\cdot H_2O$ (3)*

Reaction mixture of $MnBr_2$ (21.5 mg, 0.1 mmol), HL (25.2 mg, 0.1 mmol), 1,10-phenanthroline (18.0 mg, 0.1 mmol), and KOH (5.61 mg, 0.1 mmol) in 10 mL H_2O was sealed in a 16 mL Teflon-lined stainless steel container and heated at 140 °C for 3 days. After cooling to room temperature, pale yellow block crystals of **3** were collected by filtration and washed by water and ethanol several times with a yield of 36% based on HL. Anal. calcd for $C_{42}H_{32}N_6O_5Mn$: C, 66.75; H, 4.27; N, 11.12%. Found: C, 66.96; H, 4.16; N, 11.32%. IR (KBr pellet, cm^{-1}): 3486 (m, br), 1594 (s), 1553 (s), 1508 (m), 1457 (w), 1381 (s), 1351 (w), 1290 (w), 1260 (w), 1199 (w), 1174 (w), 1138 (w), 10,939 (w), 910 (w), 845 (m), 749 (s), 623 (w), 542 (w).

2.5. *Preparation of $[Mn_2(L)_2(phen)_4]\cdot 2ClO_4$ (4)*

Reaction mixture of $Mn(ClO_4)_2\cdot 6H_2O$ (36.2 mg, 0.1 mmol), HL (25.2 mg, 0.1 mmol), 1,10-phenanthroline (18.0 mg, 0.1 mmol), and KOH (5.61 mg, 0.1 mmol) in 10 mL H_2O was sealed in a 16 mL Teflon-lined stainless steel container and heated at 140 °C for 3 days. After cooling to room temperature, pale yellow block crystals of **4** were collected by filtration and washed by water and ethanol several times in 52% yield based on HL. Anal. calcd for $C_{78}H_{54}Cl_2N_{12}O_{12}Mn_2$: C, 61.15; H, 3.55; N, 10.97%. Found: C, 60.96; H, 3.76; N, 11.22%. IR (KBr pellet, cm^{-1}): 1597 (s), 1567 (s), 1512 (m), 1491 (w), 1456 (w), 1425 (s), 1410 (s), 1345 (w), 1284 (w), 1264 (w), 1203 (w), 1173 (w), 1142 (w), 1091 (s), 864 (w), 849 (s), 803 (w), 793 (w), 773 (w), 732 (s), 621 (m). *Caution:* perchlorate salt must be handled with care for potential explosion hazard.

2.6. *X-ray crystallography*

Crystallographic data collections for **1–4** were carried out on a Bruker Smart Apex CCD area-detector diffractometer using graphite-monochromated Mo–K_α radiation ($\lambda = 0.71073$ Å)

Table 1. Crystal data and structure refinements for **1–4**.

	1	**2**	**3**	**4**
Empirical formula	$C_{30}H_{24}N_4O_5Co$	$C_{30}H_{24}N_4O_5Zn$	$C_{42}H_{32}N_6O_5Mn$	$C_{78}H_{54}Cl_2N_{12}O_{12}Mn_2$
Formula weight	579.46	585.90	755.68	1532.11
Temperature (K)	293(2)	293(2)	293(2)	293(2)
Crystal system	Monoclinic	Monoclinic	Monoclinic	Triclinic
Space group	$C2/c$	$P2_1/n$	$P2_1/n$	$P-1$
a/Å	25.293(11)	11.465(5)	10.0679(8)	12.162(5)
b/Å	11.661(5)	16.149(5)	18.8408(15)	12.335(5)
c/Å	21.605(10)	14.953(5)	18.8349(15)	12.760(5)
α/°	90.00	90.00	90.00	95.140(5)
β/°	124.240(5)	105.257(5)	100.538(2)	113.068(5)
γ/°	90.00	90.00	90.00	91.712(5)
V (Å^3)	5268(4)	2670.9(17)	3512.5(5)	1749.7(12)
Z	8	4	4	1
D_{calc} (g cm^{-3})	1.461	1.457	1.429	1.454
$F(000)$	2392	1208	1564	786
θ range/°	1.95–27.50	1.89–28.00	2.15–25.00	1.82–27.47
Reflections collected	15,424	16,414	17,077	13,684
Independent reflections	5986	6324	6098	7870
Goodness-of-fit on F^2	1.131	1.072	1.325	1.047
R_1 $[I > 2\sigma(I)]^a$	0.0503	0.0437	0.0997	0.0582
wR_2 $[I > 2\sigma(I)]^b$	0.1293	0.1205	0.1693	0.1521

$^aR_1 = \Sigma||F_o| - |F_c||/\Sigma|F_o|$. $^bwR_2 = |\Sigma w(|F_o|^2 - |F_c|^2)|/\Sigma|w(F_o)^2|^{1/2}$, where $w = 1/[\sigma^2(F_o^2)+(aP)^2 + bP]$. $P = (F_o^2 + 2F_c^2)/3$.

at 293(2) K. The diffraction data were integrated using the SAINT program [10], which was also used for intensity corrections for Lorentz and polarization effects. Semi-empirical absorption correction was applied using SADABS [11]. The structures of **1–4** were solved by direct methods and all non-hydrogen atoms were refined anisotropically on F^2 by full-matrix least-squares using SHELXL-97 crystallographic software package [12]. In **1–4**, all hydrogens on carbons were generated geometrically. In **3**, the hydrogens on O1 W could be found at reasonable positions in the difference Fourier maps and fixed there; for **1** and **2**, hydrogens of lattice water could not be located and thus were not included in the refinement. The details of crystal parameters, data collection, and refinements for the complexes are summarized in table 1 and the details of selected bond lengths and angles are listed in table 2.

3. Results and discussion

3.1. *Preparation*

Hydrothermal reactions of stoichiometric amounts of corresponding metal with HL in the presence of KOH provided single-crystalline materials of **1** and **2** analyzed as $[Co(L)_2]\cdot H_2O$ (**1**) and $[Zn(L)_2]\cdot H_2O$ (**2**). When 1,10-phenanthroline (phen) was introduced into manganese(II) salt and HL, two manganese complexes, $[Mn(L)_2(phen)]\cdot H_2O$ (**3**) and $[Mn_2(L)_2(phen)_4]\cdot 2ClO_4$ (**4**), were successfully obtained. Complexes **1–4** are stable in air. The coordination modes of HL in **1–4** are displayed in scheme 1. In the following sections, we will describe the structures.

3.2. *Crystal structure description of $[Co(L)_2]\cdot H_2O$ (1)*

Single-crystal X-ray analysis reveals that **1** crystallizes in the monoclinic $C2/c$ space group and consists of guest waters and 2-D wave-like layers. There are a Co(II), two L^-, and

Table 2. Selected bond lengths (Å) and angles (°) for **1**–**4**.

1			
Co(1)–O(2)	2.037(2)	Co(1)–O(3)	2.016(2)
Co(1)–N(3)#1	2.079(2)	Co(1)–N(1)#2	2.067(2)
O(2)–Co(1)–O(3)	135.08(9)	O(2)–Co(1)–N(3)#1	99.10(9)
O(2)–Co(1)–N(1)#2	108.64(9)	O(3)–Co(1)–N(3)#1	109.13(10)
O(3)–Co(1)–N(1)#2	102.54(9)	N(1)#2–Co(1)–N(3)#1	95.85(10)
2			
Zn(1)–O(1)	1.951(2)	Zn(1)–N(3)	2.034(2)
Zn(1)–O(3)#1	1.980(2)	Zn(1)–N(1)#2	2.054(2)
O(1)–Zn(1)–N(3)	96.30(9)	O(1)–Zn(1)–O(3)#1	133.30(10)
O(1)–Zn(1)–N(1)#2	104.50(8)	O(3)#1–Zn(1)–N(3)	110.42(9)
N(1)#2–Zn(1)–N(3)	101.81(8)	O(3)#1–Zn(1)–N(1)#2	106.40(8)
3			
Mn(1)–N(1)	2.220(4)	Mn(1)–N(3)	2.239(4)
Mn(1)–N(5)	2.355(4)	Mn(1)–N(6)	2.357(4)
Mn(1)–O(2)#1	2.100(4)	Mn(1)–O(3)#2	2.124(4)
N(1)–Mn(1)–N(3)	178.27(17)	N(1)–Mn(1)–N(5)	91.77(15)
N(1)–Mn(1)–N(6)	88.59(15)	O(2)#1–Mn(1)–N(1)	86.65(15)
O(3)#2–Mn(1)–N(1)	91.49(16)	N(3)–Mn(1)–N(5)	89.87(15)
N(3)–Mn(1)–N(6)	91.46(15)	O(2)#1–Mn(1)–N(3)	91.62(16)
O(3)#2–Mn(1)–N(3)	88.78(16)	N(5)–Mn(1)–N(6)	70.33(15)
O(2)#1–Mn(1)-N(5)	158.64(15)	O(3)#2–Mn(1)–N(5)	99.49(17)
O(2)#1–Mn(1)–N(6)	88.33(16)	O(3)#2–Mn(1)–N(6)	169.81(17)
O(2)#1–Mn(1)–O(3)#2	101.85(17)		
4			
Mn(1)–O(2)	2.125(2)	Mn(1)–N(1)	2.241(2)
Mn(1)–N(2)	2.275(2)	Mn(1)–N(3)	2.307(2)
Mn(1)–N(4)	2.254(2)	Mn(1)–O(1)#1	2.145(2)
O(2)–Mn(1)–N(1)	92.30(8)	O(2)–Mn(1)–N(2)	164.77(8)
O(2)–Mn(1)–N(3)	86.53(7)	O(2)–Mn(1)–N(4)	94.12(8)
O(1)#1–Mn(1)–O(2)	92.46(7)	N(1)–Mn(1)–N(2)	73.61(8)
N(1)–Mn(1)–N(3)	98.92(8)	N(1)–Mn(1)–N(4)	169.41(8)
O(1)#1–Mn(1)–N(1)	100.52(8)	N(2)–Mn(1)–N(3)	89.93(8)
N(2)–Mn(1)–N(4)	99.01(8)	O(1)#1–Mn(1)–N(2)	95.74(8)
N(3)–Mn(1)–N(4)	73.10(8)	O(1)#1–Mn(1)–N(3)	160.56(8)
O(1)#1–Mn(1)–N(4)	87.63(8)		

Symmetry transformations used to generate equivalent atoms: for **1**, #1 $x,-1+y,z$; #2 $x,-y,-1/2+z$; for **2**, #1 $-1+x,y,z$; #2 $3/2-x,-1/2+y,3/2-z$; for **3**, #1 $3/2-x,1/2+y,3/2-z$; #2 $2-x,1-y,2-z$; and for **4**, #1 $2-x,1-y,2-z$.

one disordered lattice water in the asymmetric unit of **1**. As shown in figure 1(a), each Co (II) is four-coordinate with two benzimidazolyl nitrogens and two carboxylate oxygens from four different L^- to furnish a distorted tetrahedral coordination geometry [CoN_2O_2]. There are two kinds of crystallographically separate L^- with the same μ_1-$\eta^1:\eta^0$-monodentate coordination, but different molecular conformations, embodied by the different dihedral angles and the different torsion angles. Within L^- containing the central benzene C1–C6, the dihedral angle between benzimidazole and benzene ring is 82.5° and the torsion angle C3-C4-C8-N2 is 174.1°, while within another L^- containing central benzene C16–C21, the corresponding dihedral angle is 84.3° and the torsion angle C18–C19–C23–N4 is 167.8°. Each L^- bridges two Co(II) centers; each Co(II) is coordinated by four L^-. These connections extend infinitely to form a 2-D polymeric layer structure (figure 1(b)). From the perspective of topology, each Co(II) ion can be regarded

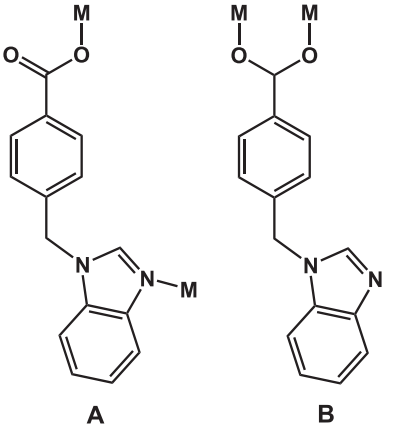

Scheme 1. Coordination modes of L^- appearing in complexes: A**, 1**–**3** and B**, 4**.

as a 4-connector and each L^- as a 2-connector simplified into a linear bridge (figure 1(c)). As a result, **1** can be simplified into a uninodal 4-connected 2-D net with the Point (Schläfli) symbol of $(4^4.6^2)$ (figure 1(d)) calculated by TOPOS [13].

3.3. *Crystal structure description of $[Zn(L)_2]\cdot H_2O$ (2)*

To investigate the impact of metal center with different coordination geometries on the structure of the assembly reaction product, $Zn(NO_3)_2\cdot 6H_2O$ instead of $Co(NO_3)_2\cdot 6H_2O$ was used to react with HL under the same reaction conditions. Complex **2** crystallizes in the monoclinic $P2_1/n$ space group. The asymmetric unit of **2** consists of one Zn(II), two L^-, and one disordered lattice water exhibiting a distorted tetrahedral coordination geometry $[ZnN_2O_2]$ (figure 2(a)). Compared with **1**, **2** exhibits the same tetrahedral coordination geometry $[MN_2O_2]$ and the same coordination modes of L^-, and thus displays similar 2-D layer structure (figure 2(b)) and topology patterns (figure 2(c) and (d)). However, obvious differences in structure of **1** and **2** were observed, reflected by the different dihedral angles and torsion angles in L^-. In **2**, for the central benzene C1–C6, the dihedral angle between benzimidazole and benzene ring is 85.8° and the torsion angle C3–C4–C8–N2 is 82.3°, while within another L^- containing central benzene C16–C21, the corresponding dihedral angle is 87.8° and the torsion angle C18–C19–C23–N4 is 167.8°. The structural diversity between **1** and **2** implies that metal cations have impact on the structure of complexes.

3.4. *Crystal structure description of $[Mn(L)_2(phen)]\cdot H_2O$ (3)*

When 1,10-phenanthroline (phen) was introduced into $MnBr_2$ and HL reaction systems, **3** was obtained. Single-crystal X-ray analysis of $[Mn(L)_2(phen)]\cdot H_2O$ reveals that **3** is composed of guest waters and 2-D wave-like layers based on Mn(II), L^- ligands, and phen in the monoclinic $P2_1/n$ space group. There are one Mn(II) ion, two L^-, one phen, and one lattice water in the asymmetric unit of **3**. As shown in figure 3(a), each Mn(II) is six-coordinate by two benzimidazolyl nitrogens, two phen nitrogens, and two carboxylate oxygens to furnish a distorted octahedral coordination geometry $[MnN_4O_2]$. The equatorial plane is occupied by two carboxylate oxygens and two nitrogens from phen and two axial positions

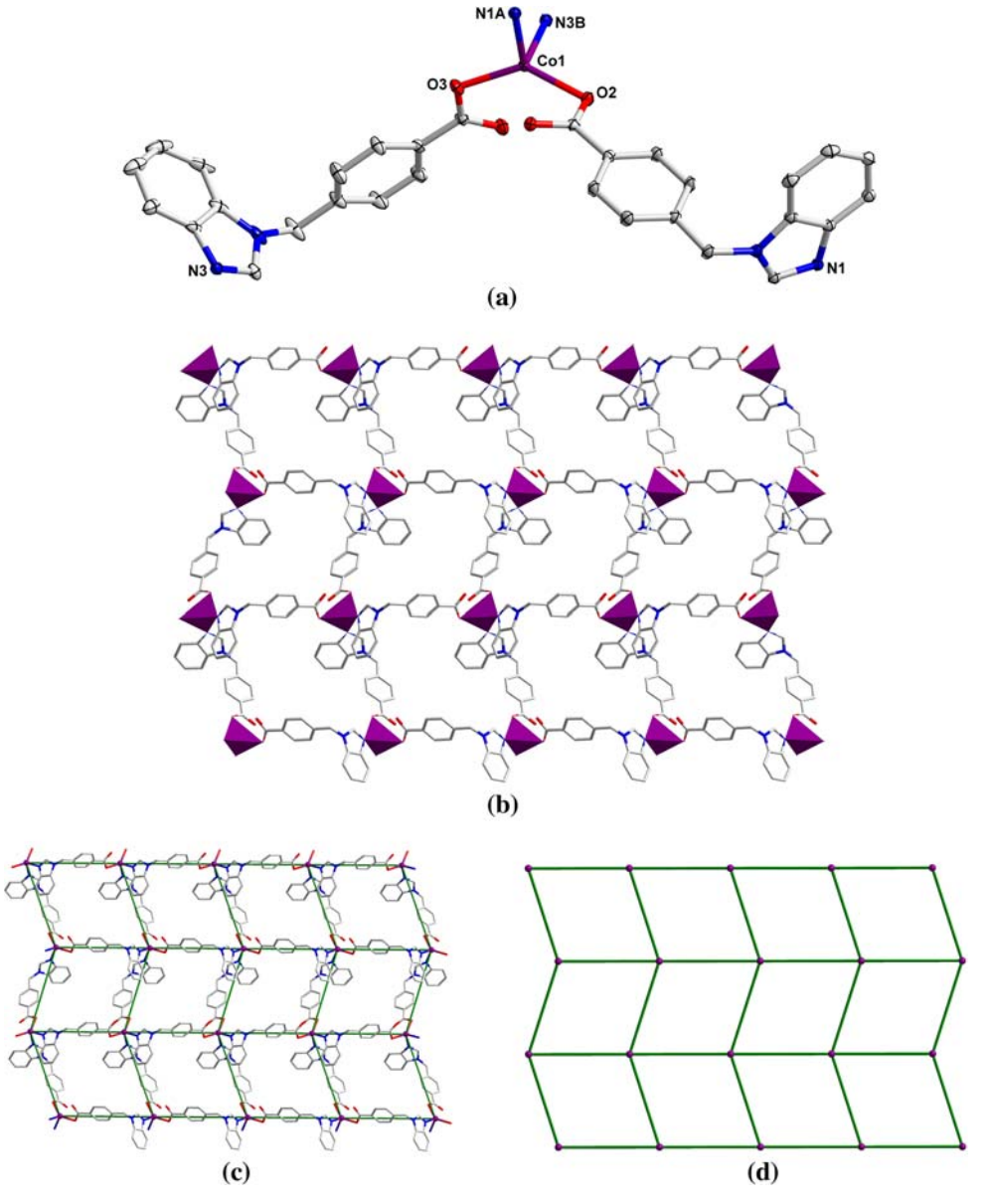

Figure 1. (a) The coordination environment of Co(II) in **1** with ellipsoids drawn at the 30% probability level. Hydrogens and lattice waters are omitted for clarity. Symmetry transformations: A, x, y, $-1/2+z$; B, x, $-1+y$, z. (b) View of the 2-D network of **1**. (c) View of the (4,4) net of **1**. (d) Schematic representation of the uninodal 4-connected 2-D net of **1** with the Point (Schläfli) symbol of $(4^4.6^2)$.

are held by two benzimidazolyl nitrogens. In **3**, there are two kinds of L^- in spite of exhibiting the same μ_1-$\eta^1:\eta^0$-monodentate coordination, which can be embodied by different molecular conformations and different functions in the construction of molecular architecture. Within L^- containing central benzene C16–C21, the dihedral angle between benzimidazole and benzene is 85.4° and the torsion angle C18–C19–C23–N4 is −54.3°. Two such L^- doubly bridge two different Mn(II) ions to form a secondary building unit

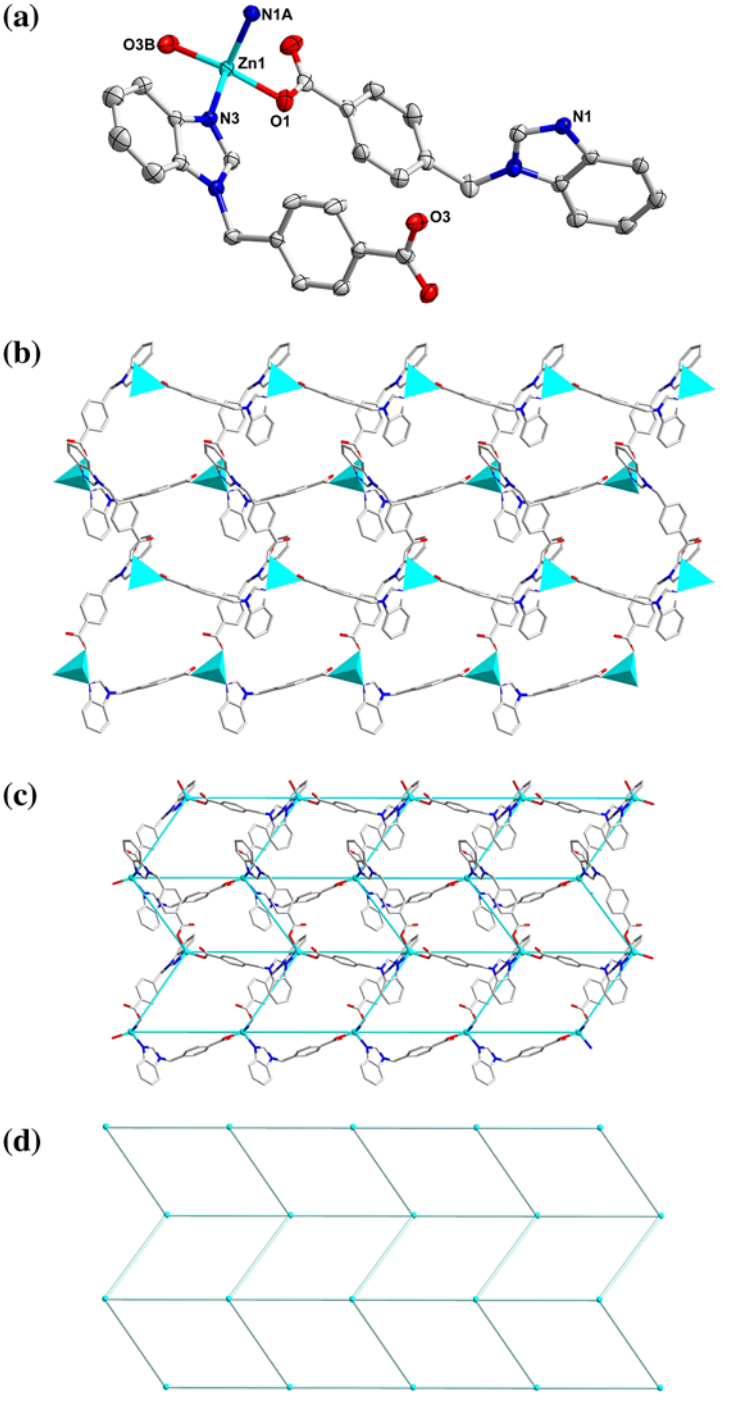

Figure 2. (a) The coordination environment of Zn(II) in **2** with ellipsoids drawn at the 30% probability level. Hydrogens and lattice waters are omitted for clarity. Symmetry transformations: A, $3/2-x$, $-1/2+y$, $3/2-z$; B, $-1+x$, y, z. (b) View of the 2-D network of **2**. (c) View of the (4,4) net of **2**. (d) Schematic representation of the uninodal 4-connected 2-D net of **2** with the Point (Schläfli) symbol of $(4^4.6^2)$.

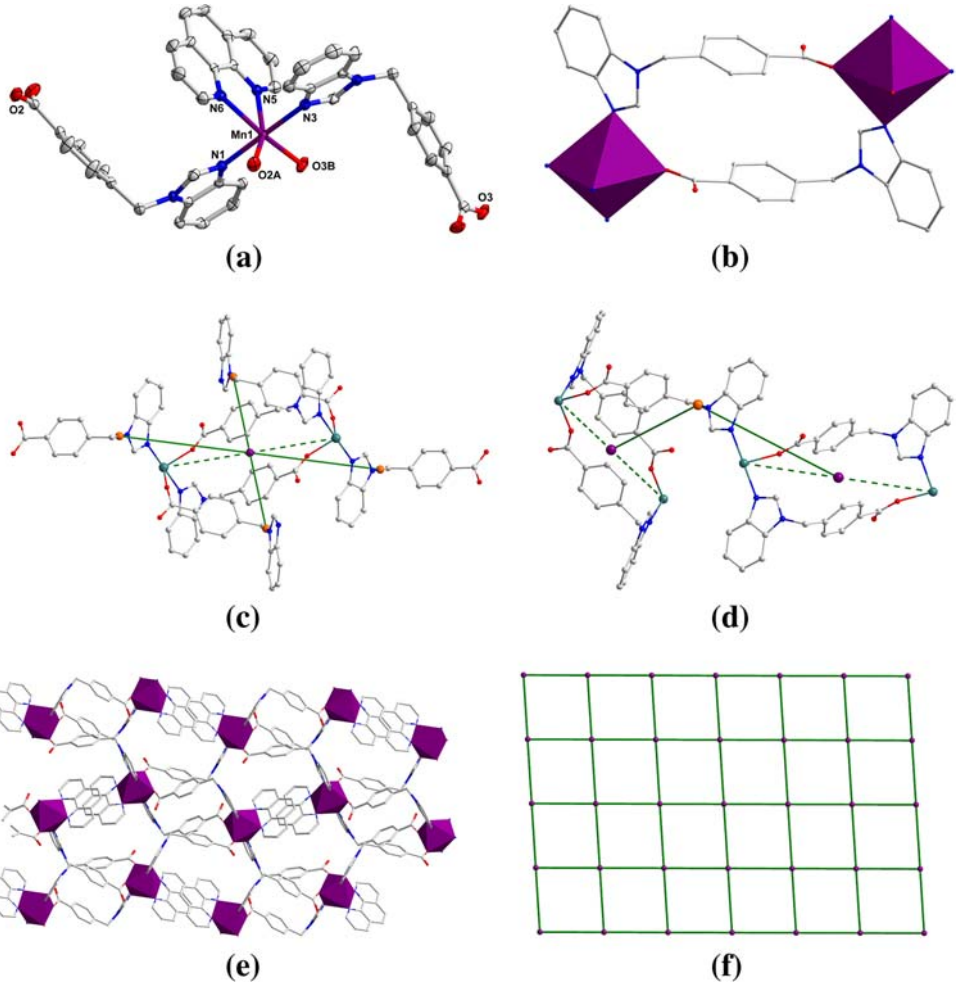

Figure 3. (a) The coordination environment of Mn(II) in **3** with ellipsoids drawn at the 30% probability level. Hydrogens and lattice waters are omitted for clarity. Symmetry transformations: A, $3/2-x$, $1/2+y$, $3/2-z$; B, $2-x$, $1-y$, $2-z$. (b) Two L^- doubly bridge two different Mn(II) ions to form a SBU $[Mn_2(L)_2]$ in **3**. (c) Schematic representation of the four-connecting node of SBU $[Mn_2(L)_2]$. (d) Schematic representation of the two-connecting node of L^-. (e) View of 2-D network of **3**. (f) Schematic representation of the uninodal 4-connected 2-D net with the Point (Schläfli) symbol of $(4^4.6^2)$.

(SBU) $[Mn_2(L)_2]$ (figure 3(b)). Within the L^- containing central benzene ring C1–C6, the dihedral angle between benzimidazole and benzene ring is 78.6° and the torsion angle C3–C4–C8–N2 is −118.7°. Such L^- as 2-connectors bridge different SBU to build the molecular frameworks. Each L^- connects two Mn(II) centers and each Mn(II) is coordinated by four L^-. This interconnection extends infinitely to form a 2-D polymeric layer structure (figure 3(e)). From the perspective of topology, each SBU $[Mn_2(L)_2]$ can be regarded as a 4-connector node to connect four different L^- containing C1–C6 (figure 3(c)) and each L^- with central benzene C1–C6 is regarded as a 2-connector node (figure 3(d)), which can be simplified as a linear bridge. Therefore, **3** is finally simplified into a uninodal 4-connected 2-D net with $(4^4.6^2)$ topology (figure 3(f)).

3.5. *Crystal structure description of $[Mn_2(L)_2(phen)_4]\cdot 2ClO_4$ (4)*

Complex **4** displays a dinuclear structure in triclinic $P-1$ space group. The asymmetric unit of **4** consists of one Mn(II), one L^-, two phen, and one perchlorate. As shown in figure 4(a), each Mn(II) is located on an inversion center and coordinated by two carboxylate oxygens from two different L and four nitrogens from two phen, exhibiting a distorted octahedral coordination geometry [MnN_4O_2]. Two carboxylate oxygens are located in the equatorial plane. The carboxylate of L^- in **4** adopts μ_2-$\eta^1:\eta^1$-bridging coordination linking two Mn(II) ions with almost identical Mn–O distance (2.125 (2) and 2.145 (2) Å, respectively). The dihedral angle between benzimidazole and central benzene ring is 66.8° and the torsion angle C27–C28–C32–N5 is −87.3°. Apart from the bonding as primary interactions, C–Hπ stacking interactions are also available: (1) between the C8–H8 and the ring of benzimidazole (symmetry code: x, $-1+y$, $-1+z$; the distance between the H8 and the centroid of benzimidazolyl plane is 2.838 Å and the angle of C8–H8···centroid is 138°); (2) between the C22–H22 and the central benzene ring of HL (symmetry code: $1-x$,

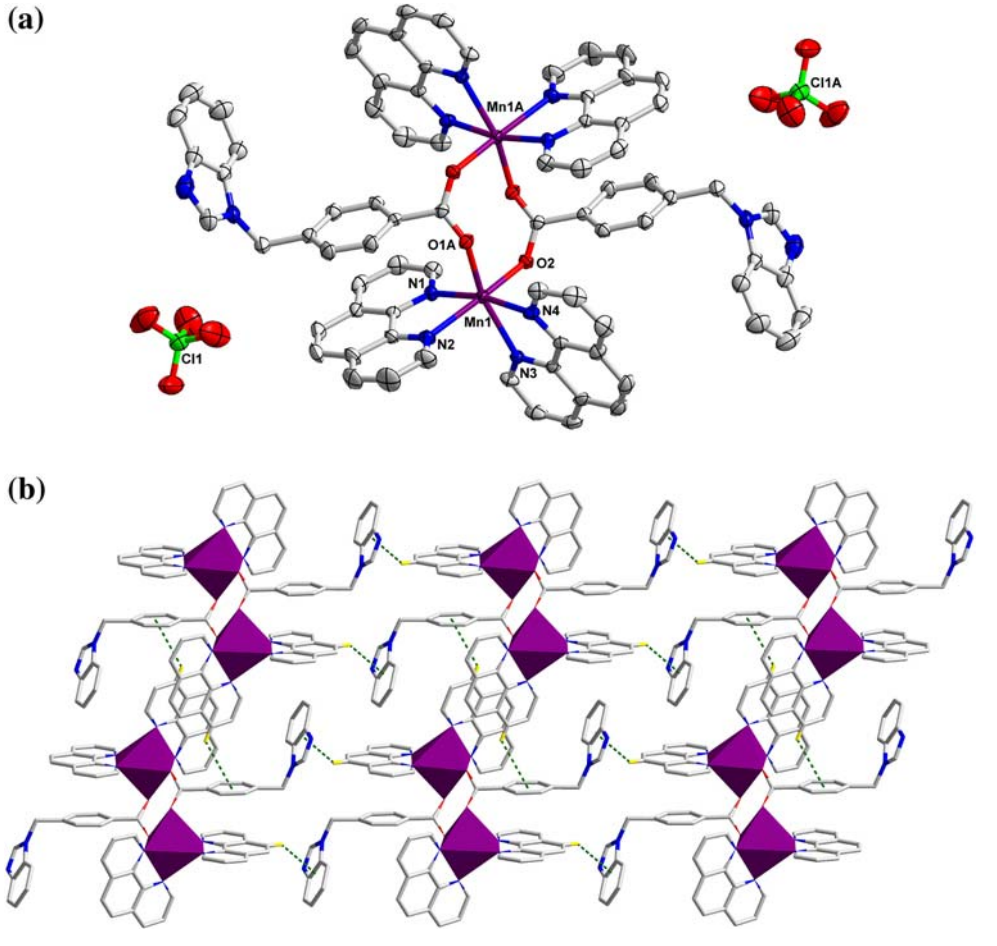

Figure 4. (a) The coordination environment of Mn(II) in **4** with ellipsoids drawn at the 30% probability level. The hydrogens are omitted for clarity. Symmetry transformations: A, $2-x$, $1-y$, $2-z$. (b) The 2-D network of **4** extended by C–H ··· π stacking interactions.

$1-y$, $2-z$; the distance between the H22 and the centroid of central benzene ring is 3.115 Å and the angle of C22–H22···centroid is 128°) [14]. These weak interactions stabilize the solid-state structure, linking different dinuclear units to yield a 2-D supramolecular network (figure 4(b)).

3.6. *PXRD, IR, and TGA*

The pure phases of **1–4** were confirmed by PXRD measurements. As shown in figure S1, each PXRD pattern of the synthesized sample is consistent with the corresponding simulated pattern.

Deprotonations of HL to give L^- in **1–4** were confirmed by crystal structures and IR spectral data (see experimental section) since no characteristic vibration bands for carboxylic group between 1680 and 1760 cm^{-1} were observed [14]. For **1–3,** the broad bands at 3400 cm^{-1} correspond to vibrations of lattice water and for **1–4,** the bands at 1500 cm^{-1} are assigned to C-H stretches of central benzene rings of HL.

Complex **4** is potentially explosive for the existence of perchlorate in its molecular structure. Thus, only **1–3** were subjected to TGA in N_2 to ascertain their thermal stabilities, from 30 °C to 800 °C (figure S2). The TGA curves reveal that **1** and **2** have similar thermal behaviors. The first step (96-156 °C for **1** and 100–189 °C for **2**) corresponds to the release of one coordinated water and the observed weight losses of 3.38% for **1** and 3.36% for **2** are very close to the calculated value (3.11 and 3.07% for **1** and **2**, respectively). The second step occurs at 381 °C for **1** and 347 °C for **2** associated with combustion of L^-. In the TGA curve of **3,** there is a weight loss of 2.26% from 92 to 141 °C, corresponding to release of one lattice water (calcd 2.38%) and from 235 to 557 °C, there is a steep weight loss assigned to decomposition of the framework. The continuous decomposition of **1–3** does not end above 800 °C, so the final residues have not been characterized.

3.7. *Photoluminescent property*

Previous studies have shown that inorganic–organic hybrid coordination polymers containing metal centers with d^{10} electron configuration such as Zn(II) exhibit excellent luminescent properties and may have potential applications as photoactive materials [15]. The photoluminescence of **2** and free HL have been investigated in the solid state at room temperature. As shown in figure 5 and S3, intense photoluminescence emission can be observed under the experimental conditions for **2** and HL with emission bands at 396 nm (λ_{ex} = 352 nm) for **2** and 393 nm (λ_{ex} = 351 nm) for HL. The fluorescent emission of **2** may be tentatively assigned to intra-ligand transition of coordinated L^- since similar emission was observed for free HL [16]. The observation of red shift of the emission maximum in **2** compared with free HL may originate from coordination [17].

3.8. *Magnetic property*

In **4**, two Mn(II) ions are bridged by carboxylates to form a dinuclear unit $[Mn_2(COO)_2]$, which might mediate magnetic interactions [18]. Therefore, the temperature dependence of magnetic susceptibility of **4** was investigated from 300 to 1.8 K with an applied magnetic field of 2000 Oe. The magnetic behavior of **4** in the forms of χ_M and $\chi_M T$ *versus* T is depicted in figure 6. The $\chi_M T$ value is 9.14 emu K mol^{-1} at 300 K. As the temperature is

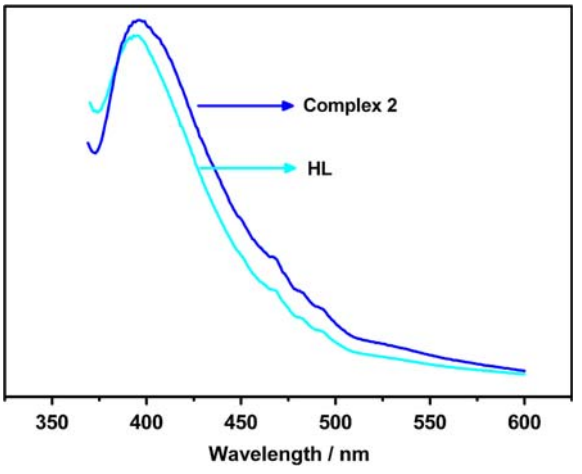

Figure 5. Emission spectra of **2** and HL in the solid state at room temperature.

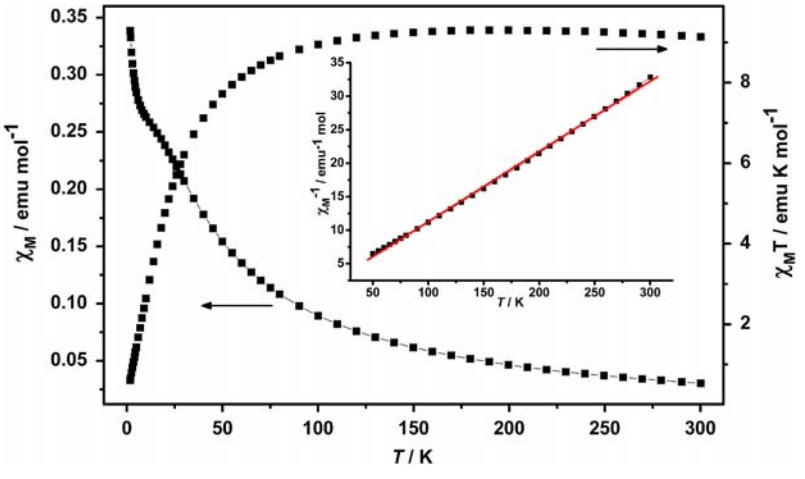

Figure 6. Temperature dependences of magnetic susceptibility of χ_M, χ_M^{-1}, and $\chi_M T$ for **4**.

gradually lowered, the $\chi_M T$ value decreases continuously with an extrapolated value which vanishes when T approaches 0, while the χ_M value increases smoothly to reach 0.339 emu mol^{-1} at 1.8 K. The $\chi_M{}^{-1}$ value (above 50 K) obeys the Curie–Weiss law with a Weiss constant (θ) of −7.37 K and a Curie constant (C) of 9.53 emu K mol^{-1}. The negative value of θ and the shape of the $\chi_M T$ *versus* T curve suggest antiferromagnetic interactions between neighboring Mn(II) centers [19].

4. Conclusions

A flexible N- and O-donor multidentate ligand 4-(benzimidazol-1-ylmethyl) benzoic acid (HL) was synthesized and employed as building blocks of frameworks. Complexes **1** and

2 were obtained via the hydrothermal reactions of HL with corresponding transition metal and analyzed as $[Co(L)_2]\cdot H_2O$ (**1**) and $[Zn(L)_2]\cdot H_2O$ (**2**). When auxiliary ligand 1,10-phenanthroline (phen) was introduced into manganese(II) salt and HL reaction systems, two new manganese complexes, $[Mn(L)_2(phen)]\cdot H_2O$ (**3**) and $[Mn_2(L)_2(phen)_4]\cdot 2ClO_4$ (**4**), were obtained. The structures of resultant complexes varied from 0-D chain to 2-D framework with different topologies. The results suggest that metal centers, auxiliary ligand, and counter anions have subtle but important influence on the structure of complexes.

Supplementary material

Crystallographic data (excluding structure factors) for the structures reported in this paper have been deposited with the Cambridge Crystallographic Data Center as supplementary publication [CCDC–864086 (for **1**), CCDC–864087 (for **2**), CCDC–864000 (for **3**), and CCDC–864001 (for **4**)]. Copies of the data can be obtained free of charge on application to CCDC, 12 Union Road, Cambridge CB2 1EZ, UK (Fax: +44 1223 336 033; E-mail: deposit@ccdc.cam.ac.uk).

Figure S1 describes the PXRD patterns of **1–4**; figure S2 shows the TGA curves of **1–4**; and figure S3 provides excitation spectra of **2** and HL in the solid state at room temperature. This supporting information for the article is available online or from the authors on request.

Acknowledgment

The authors gratefully acknowledge Huaian Administration of Science & Technology of Jiangsu Province of China (HAG2012022) for financial support of this work.

References

[1] (a) L.F. Ma, X.Q. Li, L.Y. Wang, H.W. Hou. *CrystEngComm*., **13**, 4625 (2011). (b) T. Uemura, Y. Ono, Y. Hijikata, S. Kitagawa. *J. Am. Chem. Soc*., **132**, 4917 (2010). (c) X.M. Shi, M.J. Fang, H.J. Liu, X. He, M. Shao, M.X. Li. *J. Coord. Chem*., **63**, 3743 (2010). (d) J.J. Xu, Z. Zhu, S.M. Shi, J. Zhou, C.M. Jin. J. Coord. Chem., **63**, 2296 (2010). (e) S.R. Zheng, Q.Y. Yang, Y.R. Liu, J.Y. Zhang, Y.X. Tong, C.Y. Zhao, C. Y. Su. *Chem. Commun*., 356 (2008).

[2] (a) D.E. Freeman, D.M. Jenkins, A.T. Lavarone, J.R. Long. *J. Am. Chem. Soc*., **130**, 2884 (2008). (b) J.B. Lin, J.P. Zhang, X.M. Chen. *J. Am. Chem. Soc*., **132**, 6654 (2010). (c) R. Matsuda, T. Tsujino, H. Sato, Y. Kubota, K. Morishige, M. Takata, S. Kitagawa. *Chem. Sci*., **1**, 315 (2010). (d) B. Liu, L.J. Fan, Y.Y. Liu, J. Yang, J.F. Ma. *J. Coord. Chem*., **64**, 413 (2011).

[3] (a) Y. Kobayashi, B. Jacobs, M.D. Allendorf, J.R. Long. *Chem. Mater.*, **22**, 4120 (2010). (b) Z.M. Wang, K. L. Hu, S. Gao, H. Kobayashi. *Adv. Mater.*, **22**, 1526 (2010). (c) B.H. Ye, M.L. Tong, X.M. Chen. *Coord. Chem. Rev.*, **249**, 545 (2005). (d) N.W. Ockwig, O. Delgado-Friederichs, M. O'Keeffee, O.M. Yaghi. *Acc. Chem. Res.*, **38**, 176 (2005).

[4] (a) J.R. Li, R.J. Kuppler, H.C. Zhou. *Chem. Soc. Rev.*, **38**, 1477 (2009). (b) X. Xue, X.S. Wang, R.G. Xiong, X.Z. You, B.F. Abrahams, C.M. Che, H.X. Ju. *Angew. Chem. Int. Ed.*, **41**, 2944 (2002). (c) Q. Ye, X.S. Wang, H. Zhao, R.G. Xiong. *Chem. Soc. Rev.*, **34**, 208 (2005). (d) F.Q. Wang, X.J. Zheng, Y.H. Wan, C.Y. Sun, Z.M. Wang, K.Z. Wang, L.P. Jin. *Inorg. Chem.*, **46**, 2956 (2007).

[5] (a) K.L. Zhang, Y. Chang, C.T. Hou, G.W. Diao, R.T. Wu, S.W. Ng. *CrystEngComm.*, **12**, 1194 (2010). (b) X.J. Wang, Z.M. Cen, Q.L. Ni, X.F. Jiang, H.C. Lian, L.C. Gui, H.H. Zuo, Z.Y. Wang. *Cryst. Growth Des.*, **10**, 2960 (2010). (c) L. Tang, Y.P. Wu, F. Fu, P. Zhang, N. Wang, L.F Gao. *J. Coord. Chem.*, **63**, 1873 (2010).

[6] (a) B.H. Ye, M.L. Tong, X.M. Chen. *Coord. Chem. Rev.*, **249**, 545 (2005). (b) S.S. Chen, M. Chen, S. Takamizawa, P. Wang, G.C. Lv, W.Y. Sun. *Chem. Commun.*, **47**, 4902 (2011). (c) Y.T. Wang, G.M. Tang, Y.C. Zhang, W.Z. Wan, J.C. Yu, T.D. Li, Y.Z. Cui. *J. Coord. Chem.*, **63**, 1504 (2010).
[7] (a) Y.Y. Liu, J.F. Ma, J. Yang, Z.M. Su. *Inorg. Chem.*, **46**, 3027 (2007). (b) Z.F. Tian, J.G. Lin, Y. Su, L.L. Wen, Y.M. Liu, H.Z. Zhu, Q.J. Meng. *Cryst. Growth Des.*, **7**, 1863 (2007). (c) Q. Hua, Y. Zhao, G.C. Xu, M.S. Chen, Z. Su, K. Cai, W.Y. Sun. *Cryst. Growth Des.*, **10**, 2553 (2010).
[8] (a) H.W. Kuai, X.C. Cheng, X.H. Zhu. *J. Coord. Chem.*, **64**, 1636 (2011). (b) H.W. Kuai, X.C. Cheng, X.H. Zhu. *J. Coord. Chem.*, **64**, 3323 (2011). (c) H.W. Kuai, X.C. Cheng, L.D. Feng, X.H. Zhu. *Z. Anorg. Allg. Chem.*, **637**, 1560 (2011).
[9] (a) J. Fan, B.E. Hanson. *Inorg. Chem.*, **44**, 6998 (2005). (b) G.C. Xu, Q. Hua, T. Okamura, Z.S. Bai, Y.J. Ding, Y.Q. Huang, G.X. Liu, W.Y. Sun, N. Ueyama. *CrystEngComm.*, **11**, 261 (2009).
[10] S*AINT*, *Program for Data Extraction and Reduction*, Bruker AXS, Inc., Madison, WI (2001).
[11] G.M. Sheldrick, *SADABS, Program for Bruker Area Detector Absorption Correction*, University of Gottingen, Gottingen, Germany (1997).
[12] (a) G.M. Sheldrick, *SHELXL-97*, *Programs for X-ray Crystal Structure Solution*, University of Gotinggen, Germany (1997). (b) G.M. Sheldrick, *SHELXL-97*, *Programs for X-ray Crystal Structure Refinement*, University of Gotinggen, Germany (1997).
[13] (a) V.A. Blatov, IUCr CompComm Newsletter **7**, 4 (2006). (b) V.A. Blatov. *TOPOS, A Multipurpose Crystallochemical Analysis with the Program Package*, Samara State University, Russia (2009).
[14] (a) Z. Tao, Q.J. Zhu, W.G. Jackson, Z.Y. Zhou, X.G. Zhou. *Polyhedron*, **22**, 263 (2003). (b) R.G. Lin, Z. Tao, S.F. Xue, Q.J. Zhu, W.G. Jackson, Z.B. Wei, L.S. Long. *Polyhedron*, **22**, 3467 (2003).
[15] (a) Y.B. Dong, P. Wang, R.Q. Huang, M.D. Smith. *Inorg. Chem.*, **43**, 4727 (2004). (b) D.M. Ciurtin, N.G. Pschirer, M.D. Smith, U.H.F. Bunz, H.C.Z. Loye. *Chem. Mater.*, **13**, 2743 (2001). (c) M. Chen, M.S. Chen, T. Okamura, M.F. Lv, W.Y. Sun, N. Ueyama. *CrystEngComm.*, **13**, 3801 (2011).
[16] (a) G.H. Wei, J. Yang, J.F. Ma, Y.Y. Liu, S.L. Li, L.P. Zhang. *Dalton Trans.*, 3080 (2008). (b) W. Chen, J.Y. Wang, C. Chen, Q. Yue, H.M. Yuan, J.S. Chen, S.N. Wang. *Inorg. Chem.*, **42**, 944 (2003). (c) Y.F. Han, X. H. Zhou, Y.X. Zheng, Z. Shen, Y. Song, X.Z. You. *CrystEngComm.*, **10**, 1237 (2008).
[17] (a) J.Q. Liu, Z.B. Jia, Y.Y. Wang. *J. Mol. Struct.*, **987**, 126 (2011). (b) Z. Su, J. Fan, M. Chen, T. Okamura, W.Y. Sun. *Cryst. Growth Des.*, **11**, 1159 (2011). (c) X.L. Wang, Y.F. Bi, G.C. Liu, H.Y. Lin, T.L. Hu, X.H. Bu. *CrystEngComm*., **10**, 349 (2008). (d) L. Zhang, Z.J. Li, Q.P. Lin, Y.Y. Qin, J. Zhang, P.X. Yin, J.K. Cheng, Y.G. Yao. *Inorg. Chem.*, **48**, 6517 (2009).
[18] D. Ghoshal, G. Mostafa, T.K. Maji, E. Zangrando, T.H. Lu, N.R. Chaudhuri. *New J. Chem.,* **28**, 1204 (2004).
[19] (a) M. Wang, C.B. Ma, H.S. Wang, C.N. Chen, Q.T. Liu. *J. Mol. Struct.*, **873**, 94 (2008). (b) J.W. Raebiger, J.L. Manson, R.D. Sommer, U. Geiser, A.L. Rheingold, J.S. Miller. *Inorg. Chem.*, **40**, 2578 (2001).